Title: Using total RNA quality metrics for time since deposition estimates in degrading bloodstains.

Authors: Colin I. Elliott[a,b*], Theresa E. Stotesbury[c], Aaron B.A. Shafer[a,d]

[a] Department of Forensic Science, Trent University, 1600 West Bank Drive, Peterborough, ON, K9L 0G2, Canada

[b] Applied Bioscience Graduate Program, Faculty of Science, Ontario Tech University, Oshawa, ON L1G 0C5, Canada

[c] Faculty of Science, Forensic Science, Ontario Tech University, 2000 Simcoe St N, Oshawa, ON, L1G 0C5, Canada

[d] Environmental and Life Sciences Graduate Program, Trent University, 1600 West Bank Drive, Peterborough, ON, K9L 0G2, Canada

* **Corresponding author:** colinelliott@trentu.ca

Declaration of Competing Interest

The authors report no declarations of interest.

Acknowledgements

The authors would like to thank Reni Verasztó for helping with laboratory work and data collection. The authors would also like to acknowledge Alon Gabriel, Jesse Wolf, and Marie-Laurence Cossette of the Wildlife and Applied Genomics laboratory group at Trent University for their insights and feedback on writing, visualizations, and statistical analyses. The authors also thank Otonabee Meat Packers for providing the blood samples.

28 **HIGHLIGHTS**

29 - Amplification-free analysis of total RNA in degrading bloodstains.
30 - Short-term RNA degradation assessment using high-resolution size measurements.
31 - Total RNA quality and quantity metrics were assessed across a one-week.
32 - Total RNA quality metrics demonstrated the strongest timewise trends.
33 - Biological replicates produced similar results for RNA quality metrics.

34

35 **ABSTRACT**

36 Determining the time since deposition (TSD) of bloodstains would provide forensic scientists
37 with critical information regarding the timeline of the events involving bloodshed. The
38 physicochemical changes occurring to biomolecules as a bloodstain degrades can be used to
39 approximate the TSD of bloodstains. Our study aims to quantify the timewise degradation
40 trends and temperature dependence found in total RNA from bloodstains without the use of
41 amplification, expanding the scope of the RNA TSD research which has previously targeted
42 mRNA molecules. Whole bovine blood was stored in plastic microcentrifuge tubes at 21˚C or
43 4˚C and tested over different timepoints spanning one week. Nine RNA metrics were visually
44 assessed and quantified using linear and mixed models; the RNA Integrity Number equivalent
45 (RINe) and the DV200 demonstrated strong negative trends over time and statistical
46 independence. The RINe model fit was high (R^2 = 0.60), and while including the biological
47 replicate as a random effect increased the fit for all RNA metrics, no significant differences were
48 found between biological replicates stored at the same temperature for the RINe and DV200
49 metrics. Importantly, this suggests that these standardized metrics can likely be directly

compared between scenarios and individuals, with DV200 having an inflection point at ~28 hrs. This study provides a novel approach for blood TSD estimates, producing metrics that are not affected by inter-individual variation and improving our understanding of the rapid degradation occurring in bloodstains.

KEYWORDS: RNA Integrity Number equivalent and RINe, Time since deposition and TSD, DV200, Bloodstain, Amplification-free, Aging

72 **Introduction**

73 Accurately determining the age of biological evidence, including soft tissue and bodily
74 fluids, remains a complex task in forensic investigations (1,2). Bloodstained evidence is
75 commonly observed at the scenes of crimes involving bloodshed, and determining the age, or
76 time since deposition (TSD) of a bloodstain, would provide context in criminal investigations,
77 including the development of investigative leads and the assessment of alibis (1–4). Currently,
78 bloodstains observed at crime scenes can be subjected to bloodstain pattern analysis, which
79 provides potential interpretations of the physical events that gave rise to the bloodshed (5).
80 DNA profiling, used for source attribution purposes, can be carried out from collected
81 bloodstains (6–9); however, these tools do not provide TSD estimates of blood, requiring
82 additional analyses. Bloodstains degrade in a series of complex processes, physical and
83 chemical changes are influenced by many factors, starting from the point of their formation on
84 a surface onwards (10–16). Previous studies have developed chemometric (2,13,14,17) and
85 genetic methods (3,18–20) that estimate the TSD of bloodstains in controlled laboratory
86 conditions. While these methods produce time-dependent responses, studies generally report
87 high variability in responses between samples, biological replicates and environmental
88 conditions, suggesting that the accuracy of TSD estimates might be increased by combining
89 metrics obtained from different biomolecules and/or using methods that are insensitive to
90 biological replicate variation (1,3,13,14,17–19,21).

91 *Ex-vivo*, blood undergoes a series of time-dependent physicochemical and
92 morphological changes, such as hemoglobin oxidation and conformational changes (13,22),
93 drying (12,23), clotting (24,25), and DNA and RNA degradation (3,15,26–28). Total RNA

94 encompasses ribosomal RNAs (rRNA), messenger RNAs (mRNA), transfer RNAs (tRNA) and
95 microRNAs, among others (29,30). Eukaryotic rRNA makes up for 80% of the total RNA in a cell
96 and consists of 5S, 5.8S, 18S and 28S rRNA (31). Messenger RNA expression patterns have been
97 used to identify body fluids found at crime scenes (32,33) and might also correlate with time
98 (34). Fu *et al.* (20) found that, when analyzing blood-specific mRNA transcripts, TSD for
99 bloodstains could be estimated to within a period of 2 to 6 weeks, depending on the TSD of the
100 sample. Anderson *et al.* (3) distinguished 6-day old blood from fresh and aged (30 days) blood,
101 while Lech *et al.* (18) classified deposition by three time-of-day periods with high prediction
102 accuracy. High throughput sequencing (HTS) by Weinbrecht *et al.* (19) demonstrated that
103 mRNA transcripts decreased over time, with blood-specific transcripts detected up to 12
104 months after deposition. Salzmann *et al.* (35) also used HTS to investigate the timewise changes
105 in the quality of the amplified RNA; the authors observed a marked decrease in mRNA
106 transcript integrity six months after deposition, highlighting the potential applicability of total
107 RNA quality metrics for TSD purposes (35). Collectively, these studies demonstrated the
108 timewise degradation of small RNA species in bloodstains and highlighted the surprising long-
109 term survival of RNA, supporting the applicability and implementation of techniques targeting
110 nucleic acid degradation in time series. We ask if features of quick RNA degradation can be
111 captured in the same way.

112 Most RNA studies to date have used PCR amplification to target specific mRNAs and
113 how they change in a degrading bloodstain over a long period of time (3,19,20,35). The vast
114 majority of mRNA molecules have a half-life of just minutes (36); therefore, genomic DNA
115 contamination is a concern in experiments where amplification is used to target specific mRNA

116 (37). Amplification-free analysis of RNA might provide insight into the naturally occurring RNA
117 degradation in blood without the risk of introducing any amplification biases or stochastic
118 effects seen while using RT-PCR and RT-qPCR (36,38,39). Accordingly, our study takes a holistic,
119 non-targeted and amplification-free approach by analyzing the quality (ribosomal ratios, RNA
120 integrity number equivalent; RINe, DV200) and quantity metrics (RNA size ranges, total
121 concentration, rRNA peak concentration) of total RNA in bloodstains, while simultaneously
122 quantifying the effect of temperature on RNA degradation and TSD models. Not only does
123 focusing on total RNA have the advantage of eliminating the stochastic effects and
124 amplification biases caused by reverse transcriptase and PCR, it can also circumvent potential
125 PCR inhibition from the heme in blood (38–40).

126 **Materials and Methods**

127 *Blood sample collection*

128 Bovine blood was collected from Otonabee Meat Packers, an abattoir in Peterborough,
129 Ontario, Canada. Acid dextrose anticoagulant solution A (ACD-A) was added to bovine blood at
130 a concentration of 12.5% v/v (41). Blood treated with ACD anticoagulants has demonstrated
131 better nucleic acid extraction efficiencies than heparin-based anticoagulants and has not been
132 shown to affect the cell counts of the different blood components (42). The ACD-A used in this
133 study was not shown to impact RNA metrics such as concentration and quality over time (Table
134 S1) and allowed for more accurate pipetting of the blood. ACD-A was made by dissolving 6.6
135 grams of sodium citric dextrose, 2.4 grams of citric acid, and 6.68 grams of dextrose anhydrous,
136 all purchased from ACP Chemicals Inc., in 500 mL of distilled water. Bovine blood was collected

137 in an amber Nalgene bottle containing the anticoagulant, which was subsequently placed on ice

138 for transportation back to the laboratory (approximately 15 minutes).

139 *Blood deposition*

140 50 µL of blood was deposited into 1.5 mL plastic microcentrifuge tubes. Samples were

141 left to air dry by keeping the microcentrifuge tubes lids open until RNA extraction. Samples

142 were stored at one of two temperatures: room temperature (~ 21˚C) or refrigerated at 4˚C for a

143 designated amount of time. The room temperature storage condition had an approximate 40%

144 relative humidity (RH), while the RH was likely slightly greater for samples stored at 4˚C. Five

145 time-series experiments were performed, three at 21˚C and two at 4˚C; blood from a different

146 cow (biological replicate) was used for each experiment. RNA extractions were completed at 0

147 hours (time of initial pipetting; ~ 30 minutes post-blood collection) and across various

148 timepoints (Table 1); the goal here was to compare the timewise degradation trends for blood

149 deposited at different temperatures. Five technical replicates were used for each of the

150 timepoints, resulting in a total of 200 assayed samples.

151 **Table 1.** Overview of the time series conducted and each experiment's storage temperature for

152 the bloodstains. Each biological replicate represents a different cow.

Biological Replicate	Temperature	Sample Size	Timepoints (hours after deposition)
A	21˚C	50	0,1.5,3,6,9,24,48,72,96,168
B	21˚C	50	0,1.5,3,6,9,24,36,48,72,96
C	21˚C	30	0,6,20,24,28,36
D	4˚C	35	0,3,6,9,24,48,72
E	4˚C	35	0,3,9,24,48,72,96

153

154 *RNA extraction*

155 Total RNA was extracted from the deposited blood using the PureLink Total RNA Blood
156 Purification kit by Invitrogen (43). The volume of lysis buffer (L5) recommended in the
157 manufacturer's protocol was doubled to minimize blood clotting. An optional on-column DNase
158 incubation was completed following the manufacturer's protocol. Total RNA was eluted with 30
159 µL of RNase-free water and prepared for analysis on the Agilent Technologies 4200 TapeStation
160 (44). 1 µL of the high sensitivity RNA screen tape sample buffer was mixed with 2 µL of the total
161 RNA extracts following the manufacturer's protocol for the *High Sensitivity RNA ScreenTape*
162 *Assay* (44).

163 *Automated gel electrophoresis*

164 RNA was analyzed using high-sensitivity automated gel electrophoresis with the Agilent
165 Technologies 4200 TapeStation (44). The TapeStation is a highly sensitive instrument that
166 detects RNA down to 100 pg/µl while offering a quantitative range beginning at 500 pg/µl (45).
167 It separates different-sized fragments that are tagged with an intercalating fluorescent dye by
168 automated electrophoresis, allowing for the quantification of specifically-sized RNA (45,46). A
169 ladder containing fragments of known size was also loaded next to the samples; the software
170 compared band locations and assigned 18S and 28S rRNA peaks to the RNA samples (47).

171 *RNA metrics*

172 A series of RNA metrics were collected and examined using the TapeStation Analysis Software
173 A.02.02 (Table S2). Of note, the RINe metric was generated by an algorithm that calculates the
174 ratio of the height of the 18S rRNA peak (in fluorescent units; FU) to the background RNA signal

175 (FU), which represents the signal for fragments found in the fast zone ranging from 200 bp to
176 1.8 kb (45,47). The RINe metric is a dimensionless number ranging from 1 to 10, with 10
177 representing intact and high-quality RNA, while a value of 1 represents low-quality and highly
178 fragmented RNA (45,48). Another RNA quality metric, the DV200, represents the percentage of
179 RNA fragments greater than 200 nucleotides (49). A custom RNA bin was made to estimate
180 concentration from 200 bp to 500 bp fragments, presumably representing the shorter mRNAs
181 extracted from our samples (50).

182 *Statistical analyses*

183 Correlation matrices were created prior to building models to ensure that the response
184 variables (RNA metrics) included in the analyses were not highly correlated to each other
185 (Pearson's $r < |0.70|$). Variables showing independence and a correlation to time were used to
186 build a series of linear mixed-effects models, with time (natural log-transformed) and
187 temperature as fixed effects and biological replicate (individual cow) as a random effect. An
188 interaction term between log-transformed time and the temperature was also included in our
189 models. We assigned timepoint zero a value of 0.1 (6 minutes) prior to the logarithm
190 transformation. Effect size, R^2, and p-values were recorded for each model.

191 We ran an unpaired two-sample Wilcoxon test, a non-parametric test, to determine
192 whether there was a difference in the biological replicates undergoing the same experimental
193 conditions across all timepoints (i.e. test for between-individual variance in RNA metrics). The
194 non-linearity of the RNA metrics over time was also explored by fitting non-linear curves and
195 assessing the impact on the residual standard error. We note the regressions do not require
196 shared time points between biological replicates to estimate slope, intercept, and inflection

197 points. All statistical analyses and data visualizations were created using R Version 4.0.3. Raw

198 data and scripts are publicly available and deposited at https://gitlab.com/WiDGeT_TrentU.

199 **Results**

200 We collected nine RNA metrics on 200 deposited bloodstains; four RNA metrics were

201 retained for statistical analyses as they were not correlated to each other (Pearson's r < |0.70|;

202 Fig. 1). The retained metrics included the RINe, the DV200, 28S/18S rRNA peak area ratio, and

203 total RNA concentration (Table 2).

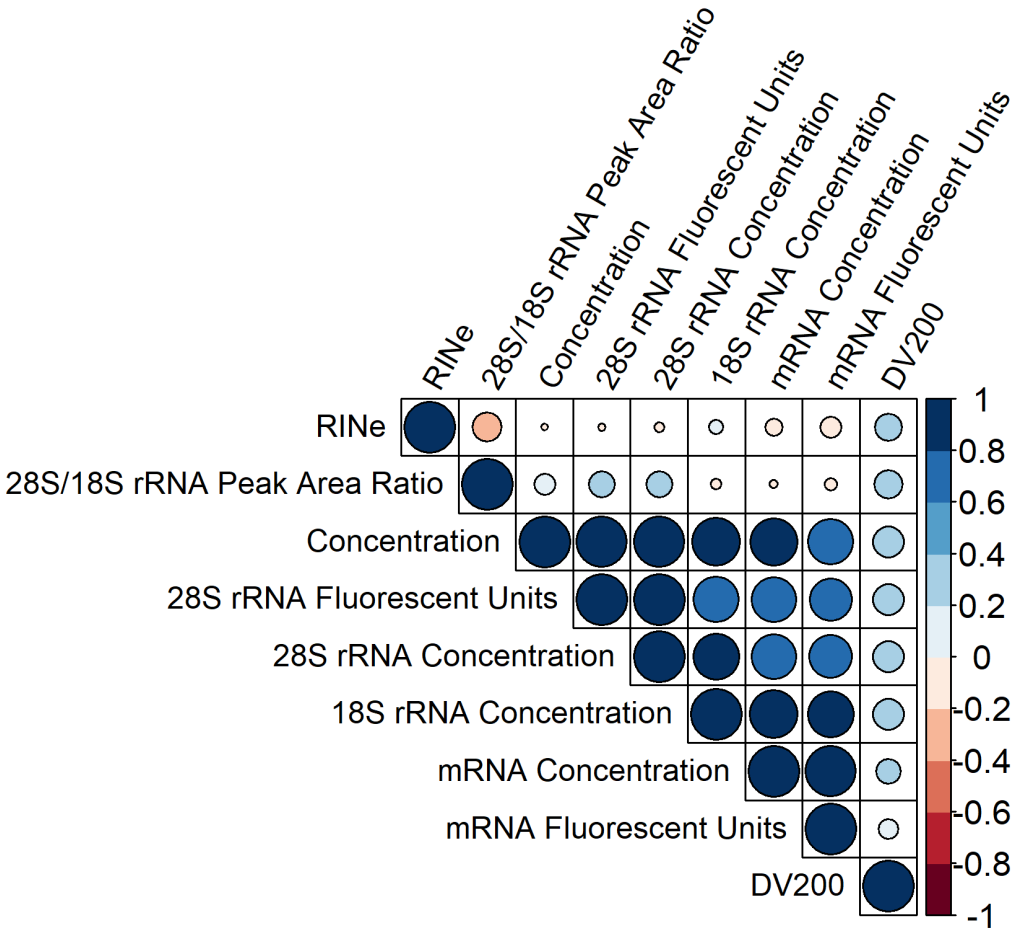

204

205 **Fig. 1 -** Correlations between the nine RNA metrics obtained from the 4200 TapeStation RNA

206 analysis. The size of the circle increases with a greater correlation between variables. Blue-

207 coloured circles indicate a positive correlation between RNA metrics, while red-coloured circles
208 indicate a negative correlation between them. The shading of the circle increases with a greater
209 correlation, with light colours indicating a weak correlation and darker colours indicating a
210 strong correlation.

211

212 **Table 2.** Statistics for the mixed models of the four quantified RNA metrics. Note that there was
213 an interaction between log-transformed time and temperature. Biological replicate was used as
214 a random effect. Each regression was computed individually for each RNA metric and each row
215 represents a separate model. Because of the interaction term, log(Time) in the table represents
216 the relationship between the response variable and time at 21˚C; Temperature (4˚C) represents
217 the difference between the intercept at both temperatures; and log(Time)*Temperature
218 reflects the difference in correlation between retained RNA metrics and time between 21˚C and
219 4˚C. P-values below 0.05 are bolded.

			log(Time)			**Temperature (4˚C)**			**log(Time)*Temperature**		
RNA metrics	**Marginal R^2**	**Conditional R^2**	**Estimate**	**Confidence Interval**	**p-value**	**Estimate**	**Confidence Interval**	**p-value**	**Estimate**	**Confidence Interval**	**p-value**
RINe	0.51	0.60	-0.51	-0.58 – -0.43	**<0.001**	0.12	-0.74 – 0.98	0.78	0.17	0.04-0.29	**0.01**
DV200	0.31	NA	-2.4	-2.99 – -1.80	**<0.001**	-0.47	-3.59 – 2.64	0.77	1.99	1.03 – 2.96	**<0.001**
28S/18S Peak Area Ratio	0.061	0.24	0.34	-0.21 – 0.89	0.22	0.35	-3.50 – 4.20	0.86	0.19	-0.54 – 0.91	0.62
Concentration	0.069	0.30	-885.42	-1305.24 – -465.60	**<0.001**	-2142.06	-7554.02 – 3269.90	0.44	789.89	116.22 – 1481.56	**0.022**

220

221

222 *RNA Integrity Number equivalent*

223 The RINe metric demonstrated the best fit model (R^2 = 0.60; Table 2) and a relationship
224 with log-transformed time (Table 2). RINe values were influenced by storage temperature,

225 however, the effect of temperature on RINe varied according to time, as seen by the significant
226 interaction effect in Table 2. The addition of biological replicate (donor) as a random effect
227 slightly increased the model's goodness-of-fit (marginal vs conditional R^2 in Table 2); this was
228 driven by a temperature-donor effect, as RINe values obtained from the different biological
229 replicates at the same temperature were not different from each other (Table 3),
230 demonstrating consistency across individuals in the same treatment. The timewise changes in
231 RINe at different temperatures (Fig. 2) showed 21˚C caused more degradation (steeper slope)
232 than the samples stored at 4˚C (Fig. 2).

233 **Table 3.** Unpaired two-sample Wilcoxon tests between the different biological replicates for the
234 RINe, DV200 and total RNA concentration. Significant p-values are bolded.

RNA metric	Biological replicate pairs	Temperature (˚C)	Test statistic (W)	p-value
RINe				
	A-B	21	1030	0.17
	A-C	21	574	0.67
	B-C	21	625	0.37
	D-E	4	335	0.36
DV200				
	A-B	21	1352	0.38
	A-C	21	658	0.14
	B-C	21	619	0.40
	D-E	4	367	0.69
Concentration				
	A-B	21	1592	**0.010**
	A-C	21	742	**0.012**
	B-C	21	626	0.36
	D-E	4	94	**<0.001**

235

236

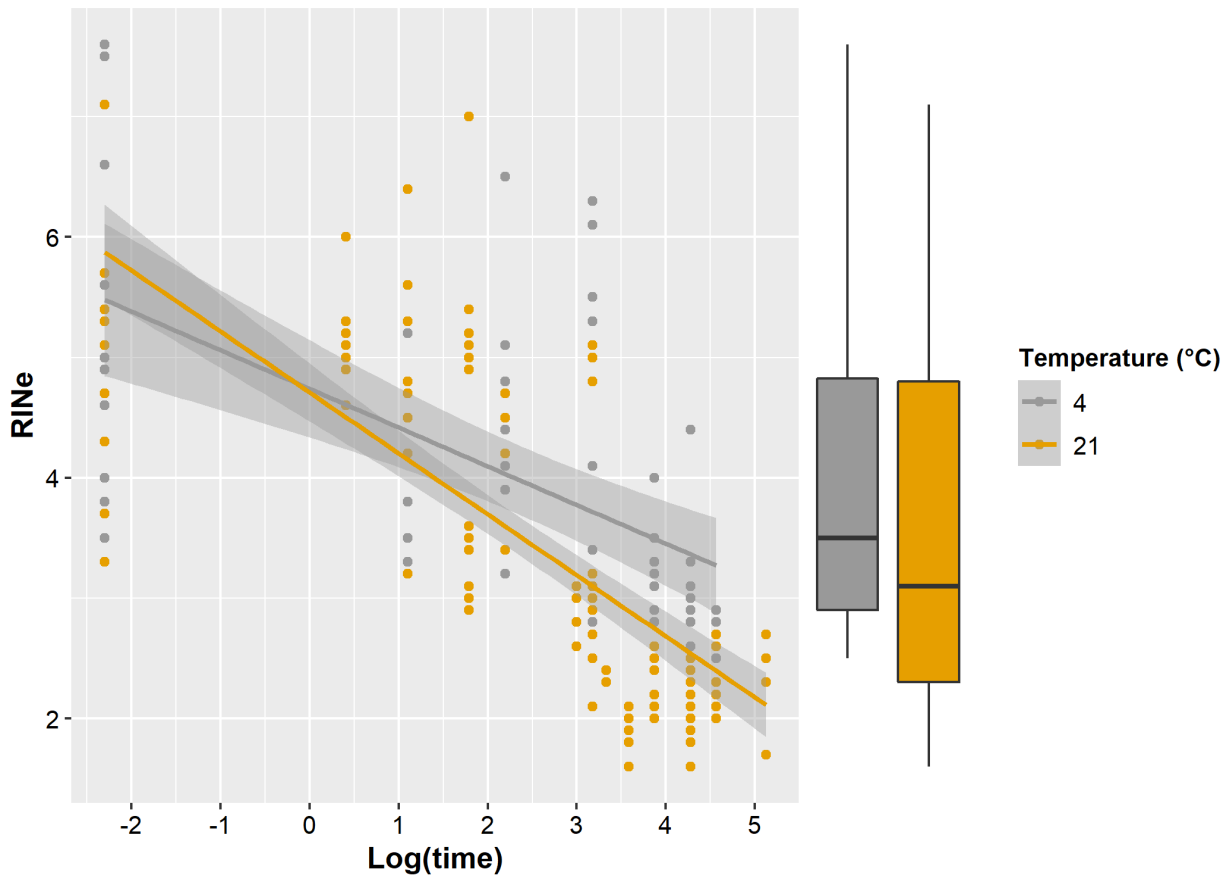

Fig. 2 - Relationship between RINe and log-transformed time (hours). RINe values are grouped by storage temperature for comparison purposes; points and regression lines are coloured according to storage temperature. Shaded areas around the regression lines represent the standard error. The interaction effect between log-transformed time and temperature is not shown as data is already separated by storage temperature.

DV200

The DV200 demonstrated the second-best model fit (R^2 = 0.31); the random effect of biological replicate did not improve the model (Table 2). DV200 showed a statistically significant relationship with time and was influenced by storage temperature, the effect of which varied according to time (Table 2). The positive estimate for the interaction effect indicated that over

248 time, bloodstains kept at 4˚C provided greater DV200 values relative to those stored at 21˚C
249 (Table 2, Fig. 3). DV200 values obtained from the different biological replicates at the same
250 temperature were not different from each other (Table 3), but there was a difference between
251 DV200 values recovered from bloodstains deposited at 21˚C and 4˚C (W = 2572, p-value =
252 0.015; Fig. 4A-B). Bloodstains stored at room temperature exhibited greater levels of
253 fragmentation over time (Fig. S1, Fig. 4A-B). DV200 values from bloodstains deposited at room
254 temperature also exhibited a non-linear trend over time; we determined that the log-logistic
255 curve – akin to a dose-response curve – provided the best fit at 21˚C. The residual standard
256 error (RSE) was smaller (5.9) in the log-logistic curve than the linear model (7.7). The inflection
257 point of the curve was at 28.1 hours (95% CI: 24.6 – 31.5 hours), suggesting a key change at this
258 time (Fig 3).

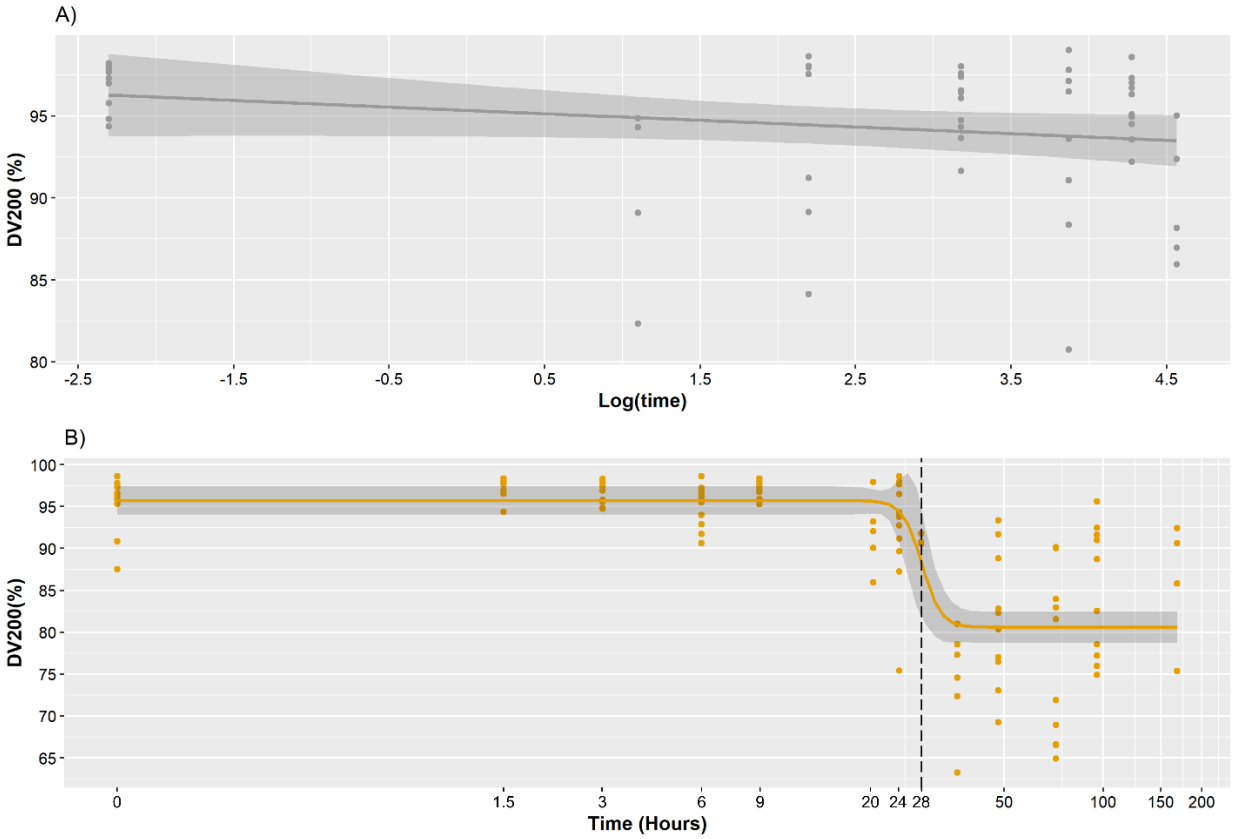

259

260 **Fig. 3 -** Relationship between the DV200 and time and temperature. **A)** Linear regression curve
261 for the DV200 against log-transformed time at 4˚C. A negative slope is observed. **B)** Log-logistic
262 curve for the DV200 against time at 21˚C. The curve displayed an inflection point at 28.1 hours,
263 indicated by the vertical dashed line. Shaded areas in **A)** and **B)** represent the standard error.
264 Note that the y-axis is scaled differently for **A)** and **B)**. The interaction effect between log-
265 transformed time and temperature is not shown.

266 *Total RNA concentration*

267 The concentration of total RNA was shown to have a lower model fit than the RINe or
268 DV200 (Table 2); the addition of biological replicate as a random effect greatly improved the
269 model's fit, suggesting high inter-individual variation (Table 2). We detected a significant
270 relationship between total RNA concentration and time and temperature (Table 2, Fig 4).
271 Importantly, we uncovered differences between concentrations from biological replicates
272 originating from the same temperature (Table 3, Fig. S2). Density plots demonstrated bimodal
273 distributions for temperature data, concordant with the result that RNA concentrations from
274 different biological replicates at the same temperature were different (Table 3, Fig. S3). Most
275 concentrations recorded for bloodstains deposited at early timepoints were above the limit of
276 quantification (500 pg/µL), while many concentrations at room temperature fell below this
277 threshold as time progressed (Fig. 4).

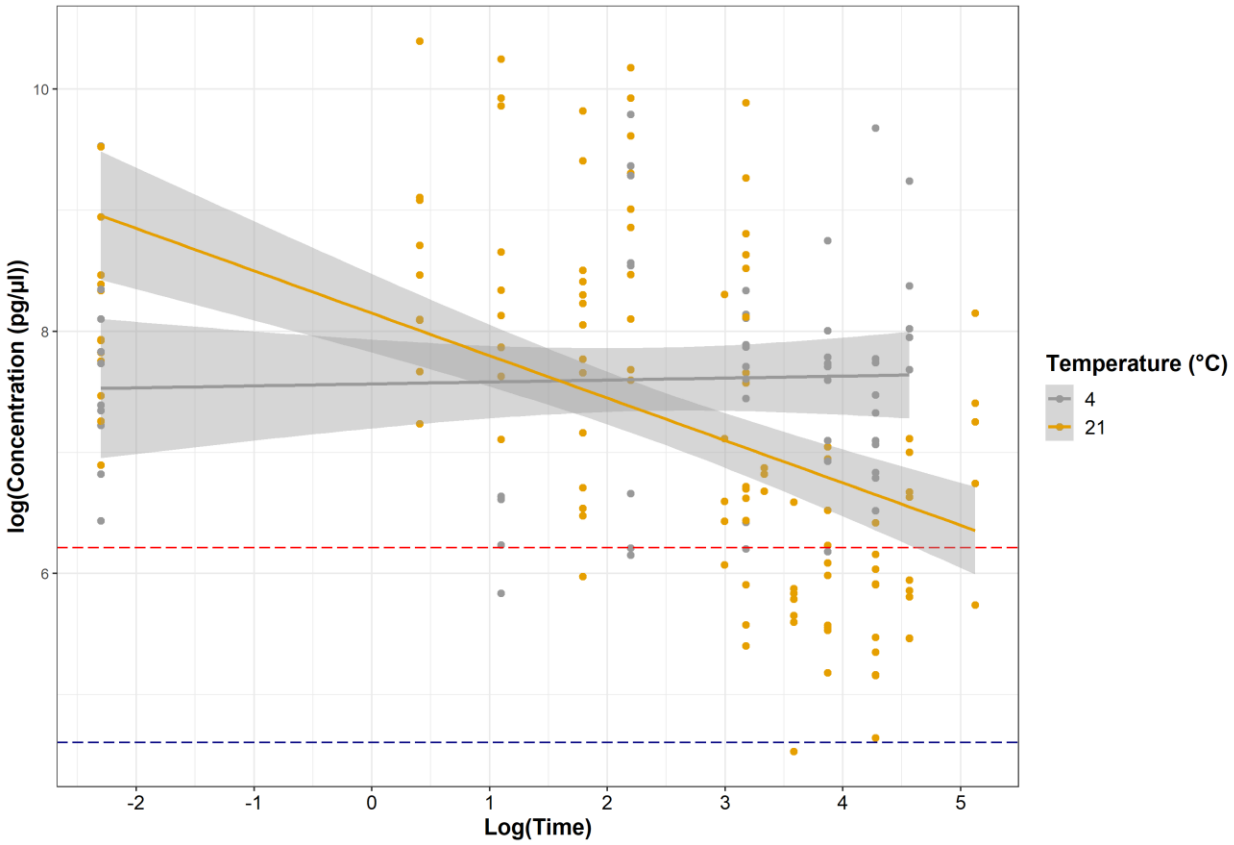

Fig. 4 – Relationships between total RNA concentration and log-transformed time (hours). Concentrations are grouped by storage temperature for comparison purposes; points and regression lines are coloured according to storage temperature. Shaded areas around the regression lines represent the standard error. Concentration was log-transformed for visualization purposes. The red dashed line represents the 4200 TapeStation's limit of quantification (500 pg/µL) and the navy dashed line represents the instrument's limit of detection (100 pg/µL).

289 *28S/18S rRNA peak area ratios*

290 The 28S/18S rRNA peak area ratio was the retained RNA metric that displayed the
291 weakest model fit and little relationship to time or temperature (Table 2). Peak area ratios were
292 only obtained for timepoints up to 24 hours for bloodstains deposited at room temperature
293 and 72 hours for those stored at 4˚C (Fig. S4); the 28S/18S peak area ratios could not be
294 obtained for the later timepoints, as the 18S rRNA peak dropped out of the electropherograms.

295 **Discussion**

296 Estimating the TSD of biological fluids found at crime scenes, such as bloodstains,
297 remains a challenge within the forensic community (1,2). Intra and inter-individual variation in
298 blood composition, substrate type and storage conditions all influence bloodstain degradation
299 and must be accounted for to accurately estimate TSD (2). This study provided a novel
300 approach to the TSD of blood, by using a non-targeted, amplification-free technique within a
301 short time since deposition period (168 hours). This is contrary to most nucleic acid studies that
302 used targeted approaches (mRNA transcripts), relied on amplification, and explored longer time
303 periods (3,19,20). Similarly to what Salzmann *et al.*(35) demonstrated using the integrity of
304 mRNA transcripts (TINe – transcript integrity number equivalent), we found that total RNA
305 quality metrics, such as the RINe and DV200, both provided clear relationships with time, with a
306 minimal effect of biological replicate on the model. A key observation here is that the limited
307 effect of biological replicate and inflection point at 28 hours of DV200 suggests these could be
308 universal diagnostic metrics.

309 The RINe is an RNA quality metric that is equal to the ratio of the 18S rRNA peak height
310 to the signal present in the fast zone (approximately 200 bp - 1.8 kb), which represents
311 fragmented RNA (45). This ratio normalized the discrepancies observed in total RNA
312 concentration and had a clear relationship to time (Fig. 2, Table 2). The addition of biological
313 replicate as a random effect in the model only marginally increased the model fit (Table 2),
314 which was driven by a temperature-donor effect (Table2, Table 3). This is important because
315 previous degradation models found a large effect of biological replicate (28), but the
316 standardized nature of RINe makes it a universally comparable metric. Blood composition varies
317 by individual, for example, research on human blood showed that the amount of RNA in
318 healthy subjects varied from 6.7 to 22.7 µg/ml (51). This variability could lead to significant
319 differences in concentrations of total RNA obtained from biological replicates, as we observed
320 during our study (Fig S2). The RINe metric was not affected by this variation (Table 2, Table 3);
321 additionally, the RINe was not highly correlated to total RNA concentration and was
322 independent of sample volume, highlighting the potential for wide-scale applicability. The
323 independent and negative correlation with time suggests the utility of RINe as a useful TSD
324 metric. We also have no reason to suspect that the patterns observed herein would not be
325 present in human blood; bovine blood has previously been optimized for forensic research
326 when acid dextrose anticoagulant solution A (ACD-A) is added at a concentration of 12.5% v/v,
327 as it exhibits similar fluid properties to that of human blood (41). Bovine blood also has a similar
328 genome size and composition to humans (52) and has similar RNA concentration (51,53), white
329 blood cell (WBC) count (human: 3.4-11.6 x 10^3/µL, bovine: 4.9-13.3 x 10^3/µL), and subtypes of
330 WBCs as human blood (neutrophils and lymphocytes are the most abundant in each organism)

331 (51,54). Confirmatory analyses validating our results using human blood could make this
332 technique applicable to crime scene samples in the future.

333 A common theme observed is the preservation effect of cold temperatures. The
334 bloodstains at 4˚C consistently demonstrated improved quality metrics when compared to the
335 bloodstains stored at 21˚C. Colder temperatures have been shown to preserve nucleic acids and
336 slow their degradation (15,16,55), a trend that was reproduced herein by comparing the slopes
337 observed in the linear models for the RINe and the DV200 (Fig. 2, Fig. 4A, Fig. S1). In both
338 instances, room temperature produced steeper slopes, indicative of faster degradation.
339 Previous studies have shown that the DV200 provides an alternative to the RINe when
340 analyzing highly degraded samples, where electropherograms lack the 18S and 28S rRNA peaks
341 due to fragmentation (49,56). The DV200 is often used as a quality indicator before library
342 preparation for high-throughput sequencing, as it is not contingent on rRNA being present to
343 provide measurements (49,57). Our results indicated that the DV200 was influenced by the
344 dropout of 18S rRNA with time (Fig. 2); specifically, the values obtained at room temperature
345 exhibited non-linear behaviour over time that appeared to be directly driven by the
346 degradation of the 18S rRNA peak occurring after one full day of exposure (Fig. 2B, Fig. S5).
347 Non-linear relationships between response variables and time have been observed in previous
348 blood TSD studies (13–15,20), indicating that non-linearity, potentially resulting from
349 preferential degradation of certain RNA fragments (or parts therein) (20), oxidation and
350 dehydration (13), is not uncommon. The non-linearity and inflection point of the DV200 values
351 at room temperature could be exploited as a diagnostic tool to differentiate bloodstains aged
352 for less than 28 hours from older ones as there is a precipitous loss of RNA that occurs at this

353 time (Fig. 2B), with most measurements approaching the instrument's limit of quantification
354 (Fig. 4), implying that little RNA is present in the sample. It is conceivable that the same curve
355 and diagnostic signature would be present at 4˚C over longer periods. Future work should
356 extend the 4˚C sampling period as this could prove useful for crime scene investigation in cold
357 climates (58).

358 As this approach analyzed total RNA rather than mRNA, direct comparisons between
359 these results and those obtained in previous studies can be difficult. Low RNA concentrations
360 were observed throughout the study, often below the limit of quantification, as time
361 progressed. The size bin ranging from 200 bp – 500 bp, which should represent the smaller
362 mRNAs in the samples, followed the same trend as total RNA and produced concentrations
363 near the limit of detection (Fig. S6). This is consistent with known half-lives of mRNA (59).
364 Although trends in total RNA degradation tend to follow those found using mRNA transcripts,
365 the latter is more sensitive as it targets a specific gene and can determine actual copy numbers
366 via amplification (3,16,20). It is also susceptible to genomic DNA contamination (37). Fu *et* al.
367 (20), and Weinbrecht *et* al. (19), both detected blood-specific transcripts from bloodstains
368 deposited for up to one year, while the total RNA concentration in this study fell below the
369 quantitative range after ~24 hours of deposition. Here, we suggest the faster degradation of
370 total RNA observed in our study allows for better discrimination at early timepoints than mRNA
371 studies.

372 **Conclusion**

373 This study demonstrated significant changes in the RINe values and a potentially
374 diagnostic inflection point in DV200 of RNA extracted from bloodstains deposited for up to 168

375 hours. The biological replicates included in this study produced similar results for the quality
376 Moving forward, in addition to an increase in sample size, longer time series at colder
377 temperatures and experiments using human blood, the effects of humidity and substrate
378 should be evaluated. These factors have been shown to affect the RNA degradation and drying
379 times of bloodstains, which could cause the clear drop in RNA metrics to occur at earlier or later
380 timepoints (16,25,60). Timewise changes in the rheological properties of blood, DNA and RNA
381 could also be explored and combined with previously developed TSD models (61,62). This type
382 of combinatorial research could bring the forensic community one step closer to developing a
383 sensitive and robust TSD model for bloodstains that could one day be applied to crime scene
384 samples.

385

386

387

388

389

390

391

392

393

Funding

This work was supported by two NSERC Undergraduate Student Research Awards (Canada) to Colin I. Elliott, Natural Sciences and Engineering Research Council of Canada, Grant/Award Number: RGPIN-2017-03934 to Aaron B.A. Shafer and RGPIN-2020-05816 to Theresa E. Stotesbury and Canadian Foundation for Innovation-JELF, Grant/Award Number: #36905 to Aaron B.A. Shafer.

412 **References**

413 1. Bremmer RH, Bruin KG De, Gemert MJC Van, Leeuwen TG Van, Aalders MCG. Forensic quest for
414 age determination of bloodstains. Forensic Sci Int 2012;216(1–3):1–11.
415 doi:10.1016/j.forsciint.2011.07.027.

416 2. Zadora G, Menzyk A. In the pursuit of the holy grail of forensic science – Spectroscopic studies
417 on the estimation of time since deposition of bloodstains. Trends Anal Chem 2018;105(5):137-
418 65. doi:10.1016/j.trac.2018.04.009.

419 3. Anderson SE, Hobbs GR, Bishop CP. Multivariate analysis for estimating the age of a bloodstain. J
420 Forensic Sci 2011;56(1):186–93. doi:10.1111/j.1556-4029.2010.01551.x.

421 4. Steelberg R, Pietro DS. A preliminary assessment of the correlation of drying time and the
422 peripheral rim thickness of perimeter bloodstains. J Forensic Res 2019;10(2):1-5.

423 5. Peschel O, Kunz SN, Rothschild MA, Mutzel E. Blood stain pattern analysis. Forensic Sci Med
424 Pathol 2011;7:257–70. doi:10.1007/s12024-010-9198-1.

425 6. Lynch M. God's signature: DNA profiling, the new gold standard in forensic science. Endeavour
426 2003;27(2):93–7. doi:10.1016/S0160-9327(03)00068-1.

427 7. Butler JM. Genetics and genomics of core short tandem repeat loci used in human identity
428 testing. J Forensic Sci 2006;51(2):253–65.doi:10.1111/j.1556-4029.2006.00046.x.

429 8. Hares DR. Selection and implementation of expanded CODIS core loci in the United States.
430 Forensic Sci Int Genet 2015;17:33–4. doi:10.1016/j.fsigen.2015.03.006.

431 9. Blackman S, Dawnay N, Ball G, Stafford-Allen B, Tribble N, Rendell P, et al. Developmental
432 validation of the ParaDNA® Intelligence System - A novel approach to DNA profiling. Forensic Sci
433 Int Genet 2015;17:137–48. doi:10.1016/j.fsigen.2015.04.009.

434 10. de Castro TC, Taylor MC, Carr DJ, Athens J, Kieser JA. Storage life of whole porcine blood used
435 for bloodstain pattern analysis. J Can Soc Forensic Sci 2016;49(1):26–37.
436 doi:10.1080/00085030.2015.1108770.

437 11. Pal A, Gope A, Iannacchione G. Temperature and concentration dependence of human whole
438 blood and protein drying droplets. Biomolecules 2021;11(2):1–18. doi:10.3390/biom11020231.

439 12. Pal A, Gope A, Obayemi JD, Iannacchione GS. Concentration-driven phase transition and self-
440 assembly in drying droplets of diluting whole blood. Sci Rep 2020;10(1):1–12.
441 doi:10.1038/s41598-020-76082-6.

442 13. Laan N, Smith F, Nicloux C, Brutin D. Morphology of drying blood pools. Forensic Sci Int
443 2018;267:104–9.

444 14. Hanson EK, Ballantyne J. A blue spectral shift of the hemoglobin soret band correlates with the
445 age (time since deposition) of dried bloodstains. PLoS One 2010;5(9):1–11.
446 doi:10.1371/journal.pone.0012830.

447 15. Doty KC, McLaughlin G, Lednev IK. A Raman “spectroscopic clock” for bloodstain age
448 determination: the first week after deposition. Anal Bioanal Chem 2016;408(15):3993–4001.
449 doi:10.1007/s00216-016-9486-z.

450 16. Cossette ML, Stotesbury T, Shafer ABA. Quantifying visible absorbance changes and DNA
451 degradation in aging bloodstains under extreme temperatures. Forensic Sci Int
452 2021;318:110627. doi:10.1016/j.forsciint.2020.110627.

453 17. Heneghan N, Fu J, Pritchard J, Payton M, Allen RW. The effect of environmental conditions on
454 the rate of RNA degradation in dried blood stains. Forensic Sci Int Genet 2021;51:102456.
455 doi:10.1016/j.fsigen.2020.102456.

456 18. Agudelo J, Huynh C, Halámek J. Forensic determination of blood sample age using a bioaffinity-
457 based assay. Analyst 2015;140(5):1411–5. doi:10.1039/c4an02269f.

458 19. Lech K, Liu F, Ackermann K, Revell VL, Lao O, Skene DJ, et al. Evaluation of mRNA markers for
459 estimating blood deposition time: Towards alibi testing from human forensic stains with
460 rhythmic biomarkers. Forensic Sci Int Genet 2016;21:119–25. doi:10.1016/j.fsigen.2015.12.008.

461 20. Weinbrecht KD, Fu J, Payton M, Allen R. Time-dependent loss of mRNA transcripts from forensic
462 stains. Res Reports Forensic Med Sci 2017;7:1–12. doi:10.2147/rrfms.s125782.

463 21. Fu J, Allen RW. A method to estimate the age of bloodstains using quantitative PCR. Forensic Sci
464 Int Genet 2019;39:103–8. doi:10.1016/j.fsigen.2018.12.004.

465 22. Strasser S, Zink A, Kada G, Hinterdorfer P, Peschel O, Heckl WM, et al. Age determination of
466 blood spots in forensic medicine by force spectroscopy. Forensic Sci Int 2007;170(1):8–14.
467 doi:10.1016/j.forsciint.2006.08.023.

468 23. Thom CS, Dickson CF, Gell DA, Weiss MJ. Hemoglobin variants: biochemical properties and
469 clinical correlates. Cold Spring Harb Perspect Med 2013; 3:1-22.
470 doi:10.1101/cshperspect.a011858.

471 24. Brutin D, Sobac B, Loquet B, Sampol J. Pattern formation in drying drops of blood. J Fluid Mech
472 2011;667:85–95. doi:10.1017/S0022112010005070.

473 25. Riddel Jr JP, Aouizerat BE, Miaskowski C, Lillicrap DP. Theories of blood coagulation. J Pediatr
474 Oncol 2007;24(3):123–31. doi:10.1177/1043454206298693.

475 26. Laber TL, Epstein BP. Substrate effects on the clotting time of human blood. J Can Soc Forensic
476 Sci 2001;34(4):209–14. doi:10.1080/00085030.2001.10757531.

477 27. Hansen J, Lesnikova I. DNA and RNA analysis of blood and muscle from bodies with variable
478 postmortem intervals. Forensic Sci Med Pathol 2014;10(3):322–8. doi:10.1007/s12024-014-
479 9567-2.

480 28. Dissing J, Søndervang A, Lund S. Exploring the limits for the survival of DNA in blood stains. J
481 Forensic Leg Med 2010;17(7):392–6. doi:10.1016/j.jflm.2010.08.001.

482 29. Stotesbury T, Cossette ML, Newell-Bell T, Shafer ABA. An exploratory time since deposition
483 analysis of whole blood using metrics of DNA degradation and visible absorbance spectroscopy.
484 Pure Appl Geophys 2020;178:735-43. doi: 10.1007/s00024-020-02494-0.

485 30. Wu J, Xiao J, Zhang Z, Wang X, Hu S, Yu J. Ribogenomics: The science and knowledge of RNA.
486 Genom Proteom Bioinf 2014;12(2):57–63. doi: 10.1016/j.gpb.2014.04.002.

487 31. Nowakowski J, Tinoco I. RNA structure and stability. Semin Virol 1997;165:153–65.

488 32. Natsidis P, Schiffer PH, Salvador-Martínez I, Telford MJ. Computational discovery of hidden
489 breaks in 28S ribosomal RNAs across eukaryotes and consequences for RNA Integrity Numbers.
490 Sci Rep 2019;9(1):1–10. doi:10.1038/s41598-019-55573-1.

491 33. Setzer M, Juusola J, Ballantyne J. Recovery and stability of RNA in vaginal swabs and blood,
492 semen, and saliva stains. J Forensic Sci 2008;53(2):296–305. https://doi.org/10.1111/j.1556-
493 4029.2007.00652.x.

494 34. Hanson E, Ingold S, Haas C, Ballantyne J. Messenger RNA biomarker signatures for forensic body
495 fluid identification revealed by targeted RNA sequencing. Forensic Sci Int Genet 2018;34:206–
496 21. doi:10.1016/j.fsigen.2018.02.020.

497 35. Bauer M. RNA in forensic science. Forensic Sci Int Genet 2007;1(1):69–74.
498 doi:10.1016/j.fsigen.2006.11.002.

499 36. Salzmann AP, Russo G, Kreutzer S, Haas C. Degradation of human mRNA transcripts over time as
500 an indicator of the time since deposition (TsD) in biological crime scene traces. Forensic Sci Int
501 Genet 2021;53:1-10. doi:10.1016/j.fsigen.2021.102524.

502 37. Chan LY, Mugler CF, Heinrich S, Vallotton P. Non-invasive measurement of mRNA decay reveals
503 translation initiation as the major determinant of mRNA stability. eLife 2018;7:1–32. doi:
504 10.7554/eLife.32536.

505 38. Hashemipetroudi SH, Nematzadeh G, Ahmadian G, Yamchi A, Kuhlmann M. Assessment of DNA
506 contamination in RNA samples based on ribosomal DNA. J Vis Exp 2018;131:1–11.
507 doi:10.3791/55451.

508 39. Minshall N, Git A. Enzyme- and gene-specific biases in reverse transcription of RNA raise
509 concerns for evaluating gene expression. Sci Rep 2020;10(1):1–7. doi:10.1038/s41598-020-
510 65005-0.

511 40. Acinas SG, Sarma-Rupavtarm R, Klepac-Ceraj V, Polz MF. PCR-induced sequence artifacts and
512 bias: Insights from comparison of two 16s rRNA clone libraries constructed from the same
513 sample. Appl Environ Microbiol 2005;71(12):8966–9. doi:10.1128/AEM.71.12.8966-8969.2005.

514 41. Sidstedt M, Hedman J, Romsos EL, Waitara L, Wadsö L, Steffen CR, et al. Inhibition mechanisms
515 of hemoglobin, immunoglobulin G, and whole blood in digital and real-time PCR. Anal Bioanal
516 Chem 2 018;410(10):2569–83. doi:10.1007/s00216-018-0931-z.

517 42. Orr A, Gualdieri R, Cossette ML, Shafer A, Stotesbury T. Whole bovine blood use in forensic
518 research: Sample preparation and storage considerations. Sci Justice 2021;61(3):214-20.
519 doi:10.1016/j.scijus.2021.02.004.

520 43. Giraldo CE, Álvarez ME, Carmona JU. Effects of sodium citrate and acid citrate dextrose solutions
521 on cell counts and growth factor release from equine pure-platelet rich plasma and pure-
522 platelet rich gel. BMC Vet Res 2015;11(60):1–7. doi:10.1186/s12917-015-0370-4.

523 44. Invitrogen Life Technologies. PureLink ™ total RNA blood purification kit: for isolating total RNA
524 from whole blood. United States, 2005.

525 45. Agilent Technologies. Agilent high sensitivity RNA screentape system quickguide. Germany
526 2015:1-4.

527 46. Agilent Technologies. Agilent 4200 TapeStation system: system manual, Germany 2019:1-212.

528 47. Agilent Technologies. Comparison of RIN and RINe algorithms for the Agilent 2100 Bioanalyzer
529 and the Agilent 2200 TapeStation systems. United States 2012:1–4.

530 48. Schroeder A, Mueller O, Stocker S, Salowsky R, Leiber M, Gassmann M, et al. The RIN: an RNA
531 integrity number for assigning integrity values to RNA measurements. BMC Mol Biol
532 2006;7(3):1–14. doi:10.1186/1471-2199-7-3.

533 49. Wimmer I, Tröscher AR, Brunner F, Rubino SJ, Bien CG, Weiner HL, et al. Systematic evaluation
534 of RNA quality, microarray data reliability and pathway analysis in fresh, fresh frozen and
535 formalin-fixed paraffin-embedded tissue samples. Sci Rep 2018;8(1):1–17. doi:10.1038/s41598-
536 018-24781-6.

537 50. Piovesan A, Caracausi M, Antonaros F, Pelleri MC, Vitale L. GeneBase 1.1: A tool to summarize
538 data from NCBI gene datasets and its application to an update of human gene statistics.
539 Database 2016;2016:1–13.doi:10.1093/database/baw153.

540 51. Chomczynski P, Wilfinger WW, Eghbalnia HR, Kennedy A, Rymaszewski M, Mackey K. Inter-
541 individual differences in RNA levels in human peripheral blood. PLoS One 2016;11(2):1–15.
542 doi:10.1371/journal.pone.0148260.

543 52. Zimin A V., Delcher AL, Florea L, Kelley DR, Schatz MC, Puiu D, et al. A whole-genome assembly
544 of the domestic cow, Bos taurus. Genome Biol 2009;10(4):1-10. doi:10.1186/gb-2009-10-4-r42.

545 53. Hammerle-Fickinger A, Riedmaier I, Becker C, Meyer HHD, Pfaffl MW, Ulbrich SE. Validation of
546 extraction methods for total RNA and miRNA from bovine blood prior to quantitative gene
547 expression analyses. Biotechnol Lett 2010;32(1):35–44. doi:10.1007/s10529-009-0130-2.

548 54. Roland L, Drillich M, Iwersen M. Hematology as a diagnostic tool in bovine medicine. J Vet
549 Diagnostic Investig 2014;26(5):592–8. doi:10.1177/1040638714546490.

550 55. Huang L, Lin P, Tsai K, Wang L. The effects of storage temperature and duration of blood
551 samples on DNA and RNA qualities. PLoS One 2017;12(9):1–13. doi:10.1371/journal.
552 pone.0184692.

553 56. Matsubara T, Soh J, Morita M, Uwabo T, Tomida S, Fujiwara T, et al. DV200 index for assessing
554 RNA integrity in next-generation sequencing. BioMed Res Int 2020;2020:1-6.doi:
555 10.1155/2020/9349132.

556 57. Illumina. Evaluating RNA quality from FFPE Samples. Guidelines for obtaining high-quality RNA
557 sequencing results from degraded RNA with Illumina RNA enrichment assays, 2016:1–4.

558 58. Historical Data - Climate - Environment and Climate Change Canada.
559 https://climate.weather.gc.ca/historical_data/search_historic_data_stations_e.html?searchTyp
560 e=stnProv&timeframe=1&lstProvince=&optLimit=yearRange&StartYear=1990&EndYear=2021&
561 Year=2021&Month=3&Day=3&selRowPerPage=25 (accessed June 30, 2021).

562 59. Baudrimont A, Voegeli S, Viloria EC, Stritt F, Lenon M, Wada T, et al. Multiplexed gene control
563 reveals rapid mRNA turnover. Sci Adv 2017;3(7):1-12. doi:10.1126/sciadv.1700006.

564 60. Sirker M, Schneider PM, Gomes I. A 17-month time course study of human RNA and DNA
565 degradation in body fluids under dry and humid environmental conditions. Int J Legal Med
566 2016;130(6):1431–8. https://doi.org/10.1007/s00414-016-1373-9

567 61. Baieth HEA. Physical parameters of blood as a non-Newtonian fluid. Int J Biomed Sci
568 2008;4(4):323–9.

569 62. Boukany PE, Wang S-Q. Shear banding or not in entangled DNA solutions depending on the level
570 of entanglement. J Rheol 2009;53(1):73–83. doi:10.1122/1.3009299.

571